J Fusion Energ
DOI 10.1007/s10894-015-0014-5

ORIGINAL RESEARCH

Parametric Optimisation of Plasma Focus Devices for Neutron Production

L. K. Lim[1] · S. L. Yap[1] · L. H. Lim[1] · Y. S. Neoh[1] · M. Z. Khan[1] · S. K. Ngoi[1] · S. S. Yap[2,3] · S. Lee[1,4,5]

Abstract A large number of experimental investigations have been carried out on plasma focus devices especially at low energy level of several kJ or over 100 kJ. There are few machines operating in the middle energy range of 10–50 kJ, where the neutron yield typically in the order of 10^8–10^9 per shot. This paper reviews the optimisation process of two different plasma focus devices (12 kJ) by applying the Lee model code. The neutron yield (Y_n) versus pressure (P) curve for several configurations of the two plasma focus provided insight of geometrical optimisation. Measured discharge current is fitted as the first step of modelling to correctly simulate the plasma dynamics. Subsequently the code is used to simulate the neutron yield of the two plasma focus devices based on beam target mechanism. Good agreement between the computed results of neutron yield versus pressure and the measured yield versus pressure is found up to the pressure where highest neutron yield is obtained. Computed highest neutron yield for most of the configuration typically differ by a factor <2.

Keywords Beam-plasma target · Lee model code · Neutron production mechanism · Neutron yield · Plasma focus

✉ S. L. Yap
yapsl@um.edu.my

[1] Physics Department, Plasma Technology Research Centre, University of Malaya, 50603 Kuala Lumpur, Malaysia

[2] UMPEDEC, University of Malaya, 50603 Kuala Lumpur, Malaysia

[3] Faculty of Engineering, Multimedia University, 63100 Cyberjaya, Selangor, Malaysia

[4] INTI International University, 71800 Nilai, Malaysia

[5] Institute for Plasma Focus Studies, 32 Oakpark Drive, Chadstone 3148, Australia

Introduction

The Dense Plasma Focus (DPF) device produces electromagnetically pinched plasma. The intense plasma emits neutrons by deuterium gas, thus the device also serves as a useful tool for the study of plasma fusion [1]. Due to the simplicity in design and operation, plasma focus device has attained considerable interest mainly for its high neutron yield in the application of intense pulse neutron sources when operated in deuterium filling [2, 3]. Moreover, it is also a rich plasma-based source of radiations, including ion, electron beams, soft and hard X-rays which are emitted from the resultant effect of extreme conditions upon plasma pinching [4–6]. The mechanism related to neutron production in the plasma focus is rather complex and still not fully understood. Technically, this is due to the transient phenomena occurring in the pinched plasma having short lifetime of 200–300 ns [7] for large devices and even shorter lifetimes for smaller devices, the lifetime scaling linearly with anode radius [8]. These short lifetimes make the diagnostics of the plasma dynamics and radiation and their correlation with existing models very challenging. In the light of these facts, research on neutron production mechanism remain active in the search for a better understanding of the neutron emission characteristic as well as physical phenomenon taking place in the neutrons generation.

Mather, pioneer of the "Mather type" plasma focus has obtained experimentally neutron yield of more than 10^{10} per shot using pure deuterium filling [7]. His early

Published online: 29 September 2015

works referred to thermonuclear origin of the neutron emission. However, Bernstein suggested that the experimental observed neutron emission was inconsistent with the thermonuclear assumption [9]. Abundance of results later also showed non-thermonuclear origin in the neutron emission [10–12]. A research group even reported that the presence of anisotropy in the neutron emission could not be interpreted solely by any single proposed model [13].

Neutron emission from the PF 1000 at 500 kJ was measured at 10^{11} n/shot [14] while a neutron burst of 10^{9} in a smaller 12 kJ plasma focus device was observed in University of Malaya [15]. Some other experiments to optimize the performance of the plasma focus device so as to obtain higher and reproducible neutron emission were also reported in order to study the neutron production mechanism in better detail. Serban and Lee [16] investigated the effect of anode geometry on the neutron yield. They employed a double-stage stepped anode configuration with speed enhancement region. Maximum axial speeds of 1.5×10^{5} m/s (15 cm/μs) was achieved and the neutron emission was found to be dependent on sheath velocity. They proposed a neutron scaling law of $Y_{th} \propto (IV)^{4}$ where Y_{th} is the thermonuclear neutrons, I is the peak discharge current and V is the peak axial speed.

Later, Koh et al. [17] enhanced the neutron yield by varying the anode and insulator sleeve length combinations, deuterium gas pressures and charging voltages. A neutron yield of $(7 \pm 1) \times 10^{8}$ n/shot was obtained at 20 mbar which has shifted the operation to high pressure regime rather than conventional reported pressure range of 3–6 mbar. The yield has been increased six-fold compared to other device operated at the same energy storage of 2 kJ. Measurement of the neutron emission showed the anisotropy factor of 1.46 ± 0.28 and suggested beam-plasma target may be the predominant mechanism in neutron production.

Verma [18] reported the effect of tubular and squirrel cage type cathode structure on the plasma focus performance for the study of neutron emission. Squirrel cage type was found to perform better over tubular type cathode with maximum average neutron yield of $(1.15 \pm 0.2) \times 10^{6}$ and $(1.82 \pm 0.52) \times 10^{5}$ n/shot, respectively. The tubular type cathode structure has an increased cathode boundary layer which produced enhanced channel choking effect of the axial phase flow which reduces the overall performance of the plasma focus device. Similar effort was made by Hussain et al. [19]. That study was on the effect of anode shape to the neutron emission from 2.7 kJ plasma focus device. A 25 % increase in neutron yield to a recorded value of 1.3×10^{8} per shot was reported using tapered anode compared to cylindrical anode shape. Hussain et al. also reported that 36 % of the input energy has been converted to pinch energy with tapered anode.

Bures et al. [20] showed by altering the anode geometry and adding inert gas to the deuterium working gas could enhance the neutron emission. Comparison of the neutron emission from pure deuterium filling, deuterium-argon-krypton admixture using cylindrical and conical anode was examined. Deuterium with inert gas admixture showed a 3–4 times increase in neutron yield using cylindrical anode shape compared to that of pure deuterium filling. However, with pure deuterium filling the conical anode shape showed a better performance at a remarkable five-fold increase in the neutron yield over the cylindrical anode. Similar work on the influence of the inert gas admixtures to the neutron production was also reported by Talaei and Sadat [21]. Recently, Verma et al. [22] demonstrated an increase in the neutron yield from a fast miniature plasma focus device of 200 J operated in high repetition rate. Neutron yield of $(1.4 \pm 0.6) \times 10^{6}$ n/s under 1 Hz operation was enhanced to one order of magnitude higher ($\sim 10^{7}$) at higher repetition rate of 10 Hz with pure deuterium filling. Higher and better reproducibility in neutron emission per shot was obtained with repetitive mode over single shot mode operation.

Potter [23] first modelled the dynamical formation and structure of the plasma focus using two-fluid MHD model. The neutron yield calculated based on the thermonuclear mechanism showed a qualitative agreement with the experimental measured D–D neutron yield. However, the model did not explain the discrepancy of the neutron yield anisotropy measured in most plasma focus discharges. Moreno et al. [24] and Gonzalez et al. [25] also computed the neutron yield based on the thermonuclear fusion mechanism and they tuned the parameters of axial and radial mass sweeping factors by comparing with measured neutron yield. In their modelling, the shock speed has been overestimated by a factor of two and leads to an increase of shock temperature by a factor of four which is too high in realistic. The thermalized D–D fusion cross section shall be increased by a factor exceeding 1000. The overestimated shock speed was due to the exclusion of the feature of 'communication delay' between the shock front and driving magnetic piston in the radial plasma slug [26].

In this paper, the behaviour of neutron emission versus pressure for different electrode geometries obtained experimentally are compared to numerical simulated results using Lee model code [27]. The Lee model code incorporated the crucial feature of 'communication delay' between the shock front and driving magnetic piston to give realistic yield of neutron from the deuterium plasma. Four model parameters; axial and radial mass factors, axial and radial current factors have been obtained by

fitting the computed current waveform against measured current waveform. In the past, extensive numerical experiments using Lee model code has been applied for the modelling of soft X-ray scaling law [28], neutron scaling law [29] and in most recent years for the modelling of ion beam properties [30–32]. In this paper, we gain further insight related to the neutron production mechanism for the 12 kJ plasma focus device. This demonstrated the versatility and utility of the Lee model code to provide a reference point in optimize plasma focus performance for neutron emission in future experiments.

Procedure Used in the Numerical Experiments

Lee model code is applied to configure the two 12 kJ plasma focus devices: UMDPF1 and UMDPF2. Experimentally measured total current waveform, the capacitor bank parameters, the focus tube parameters and the operational parameters are input to the Lee model code. Four model parameters, the mass swept-up factor f_m, plasma current factor, f_c for the axial phase, then factors f_{mr} and f_{cr} for the radial phase are adjusted sequentially to give a matching current waveform. Firstly, the axial phase model parameters are adjusted until the computed rising slope of the current waveform and peak current are in reasonable fit with the measured current waveform. We use the 5-phase code which fits the dip up to the end of the radial phase by adjusting radial phase model factors. We do not attempt to fit the current trace beyond the end of the computed current dip.

Measurement of the discharge current has always being one of the fundamental diagnostic in the plasma focus device and serves as the indicator of gross performance of the focusing plasma. Therefore, the fitting of the measured current waveform through numerical approach using Lee model code could provide a lot of valuable insights of the pinched plasma. When the fit is completed, we have the four model parameters for the specific plasma focus devices. Numerical experiment is then carried out at different pressures of deuterium filling giving the Y_n at each pressure. The computed Y_n versus P curve is then compared with the measured Y_n versus P curve. Other important information that is quickly available from the numerical experiments includes the dynamic, electrodynamics and thermodynamic properties in the various phases of the plasma focus. The code also outputs some radiation properties of the pinch phase including radiation yields in various gases, fast ion beam (FIB) and fast plasma stream (FPS) properties and neutron yields when operated in D or D-T mixtures.

Results and Discussions

The Dense Plasma Focus Device: UMDPF1

Optimization of neutron emission from the UMDPF1, a 12 kJ plasma focus device reported in a thesis [33] is reviewed. A corresponding parametric study is now being constructed with Lee model code and the numerical results obtained are to be compared with the measured results. The model parameters are determined based on the current waveform for a 20 kV shot obtained from the archived thesis.

Numerically, the UMDPF1 is configured with the following bank, tube and operating parameters according to the information in the thesis [33]:

Bank parameters	$L_0 = 52$ nH, $C_0 = 62$ μF, $r_0 = 3.2$ mΩ
Tube parameters	a = 2.5 cm, b = 5 cm, $Z_0 = 19$ cm
Operation parameters	$V_0 = 20$ kV, $P_0 = 3$ Torr, MW = 4, A = 1, At-Mol = 2

The computed current waveform fitted to the measured current waveform with good match up to the end of the computed current dip shown in Fig. 1. The fit is reasonable for the important regions of the topping profile, the top profile and the current dip except that the measured current dip shows a region of 'extended' dip which the code does not emulate. The fitting is completed to the end of the computed current dip (computed end of pinch) and no attempt is made to fit beyond that point. That there is an 'extended dip' (ED) in the measured current waveform indicates that the UMDPF1 may exhibits some Type-2

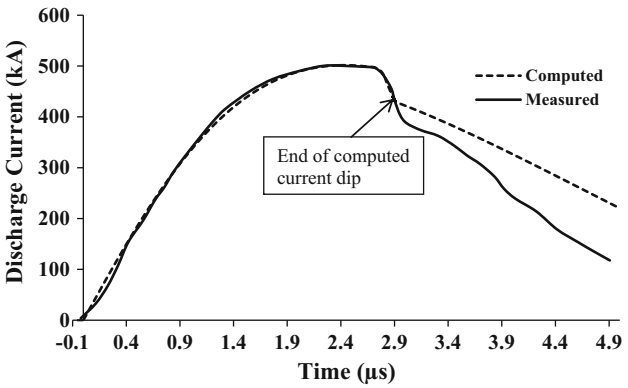

Fig. 1 Measured and computed current waveform for UMDPF1 at pressure of 3 torr. The *arrow* shows the end of the computed current dip which corresponds to the end of the computed pinch phase. The 5-phase code considers the current waveform up to this *arrowed point*. The fitting is not considered beyond this *arrowed point*

(high inductance plasma focus) characteristics due to anomalous resistance. The possible mechanism responsible for ED has not been incorporated in the Lee Model code which we are using. The anomalous resistance in the order of 1 ohm is commonly reported [34, 35]. Some characteristics of the anomalous resistance have been discussed in a recent publication [36].

From this fit, the model parameters are found and tabulated in the Table 1 below:

Using these model parameters for the series at different pressures, the model is then used to compute the neutron yield, Y_n by the beam-target mechanism [37] due to the diode action. The computed Y_n versus P curve is then plotted and compared with the measured Y_n versus P curve.

Numerical experiments on the optimization of the electrode parameters for neutron yield have been configured through a series of steps following the main steps of the original laboratory optimization experiments [33]. A summary of the steps of the physical optimization is tabulated in the Table 2.

The measured Y_n versus P for the four sets of electrode parameters are given in Fig. 2 together with the four corresponding sets of computed Y_n versus P for comparison. Features of interest for the comparison include peak Y_n, optimum pressure and the drop-off of Y_n on both sides of the optimum. As shown in the figure, the four computed neutron yield versus pressure curves agree reasonably with the measured results of the four sets of neutron yield versus pressure curves. There are several features of agreement between the computed and measured neutron yield versus pressure curves. The peak value of neutron yield drops from configuration 1 to configuration 2, and then rises in configuration 3 and further to configuration 4. The computed and measured peak values of neutron yield are in close agreement for all the four configurations. The peak value of neutron yield shifts to higher operating pressure from configurations 1–4 for the computed neutron yield versus pressure. This trend is in agreement with the measured trend.

The main point of disagreement between the computed and measured results is that the measured neutron yield versus pressure curve has a much wider spread towards the higher pressure side. There is reasonable agreement between the computed and measured curve in each case for the low pressure rising part of the neutron yield versus pressure curve. However, the measured neutron yield versus pressure curve peaks more sharply than the computed curve. The computed curve tends to peak less sharply and only reaches the measured value at a higher pressure in each case. Then, as the measured neutron yield versus pressure curve comes down as pressure is increased, the computed curve peaks at higher pressure than the measured curve and continues to drop-off much more slowly than the measured; thus exhibiting in each of the four cases a broader higher pressure curve than the measured curve.

Table 1 Four model parameters obtained from the fitting of current waveform

f_m	f_c	f_{mr}	f_{cr}
0.16	0.7	0.35	0.7

Table 2 Summary of steps to optimize the neutron yield from UMDPF1

Optimization steps	z_0 (cm)	a (cm)	b (cm)
1	18	2.5	5.75
2	18	1.25	5.75
3	16	1.25	5.75
4	16	1.25	4.25

z_0 is the anode length, a is the anode radius, b is the cathode radius, L_0 is the static inductance kept at 52 nH; C_0 is the bank capacitance kept at 62 μF, V_0 is the charging voltage kept at 20 kV, r_0 is the stray resistance kept at 3.2 mΩ; f_m, f_c, f_{mr} and f_{cr} are the four model parameters kept at values given in Table 1

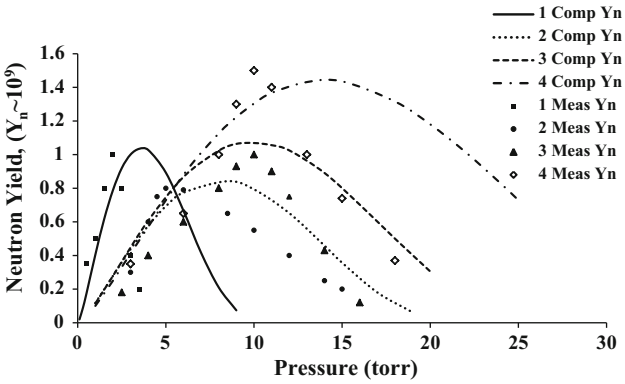

Fig. 2 Computed neutron yield versus pressure compared with measured data of UMDPF1

The Dense Plasma Focus Device: UMDPF 2

The UMDPF2 used the capacitor bank known as the Juelich I [38] (which uses wide closely spaced rigid plates for connecting the paralleled capacitors to the device thus achieving the lowest possible static inductance). Numerical experiments on the neutron yield from the UMDPF2 were also investigated using Lee model code. In this series of numerical experiments, the bank and electrode configuration is kept constant and the operational voltage, V_0 is changed from 20 to 27 kV and then to 33 kV for the optimization purpose. We have not been able to find a current trace for UMDPF2 recorded in the thesis [33]. This was because the Juelich I capacitor bank had been

converted for vacuum spark experiments, and was for a short period of time re-converted for operation of UMDPF2 for the expressed objective to test the effect of faster rise time on neutron yield. In those circumstances all neutron yield data was recorded as focus parameters and operational parameters were changed [33] but unfortunately no record of current waveforms can now be found. The design of the UMDPF2 was very similar to that of the UMDPF1 in terms of materials of electrode, insulator and chamber and in general constructional features. The main differences involved the way the collected plates were coupled to the capacitor bank. In the case of UMDPF2 these plates were directly coupled to the Juelich capacitor bank to suit its all-parallel plate low-inductance design; whereas the collector plates of UMDPF1 was coupled to the UM capacitor bank using a system of parallel coaxial cables. Thus the UMDPF2 had a plasma focus tube which was exactly the same as the UMDPF1, the difference lying only in the capacitor bank and method of coupling. Because of this we use as an approximation the same model parameters for the UMDPF2 as were fitted for the UMDPF1 (see Table 1). This approach has some justification in view of recent published results [39] which were able to establish common values for the measured model parameters of two similar machines, one in Syria and the other in Malaysia. A summary of the optimization process is tabulated in Table 3.

The measured neutron yield versus pressure for each of the three cases is shown in the Fig. 3 with comparison of the corresponding computed neutron yield versus pressure. It is seen that the computed neutron yield versus pressure curve shows similar features of agreement with the measured neutron yield versus pressure curve as already noted for the case of UMDPF1. The main features of comparison include peak neutron yield, optimum pressure and the drop-off of neutron yield on both side of optimum pressure. The computed peak neutron yield is observed to be less than the measured value. The largest difference is at 20 kV with the computed optimum neutron yield being 1/3 that of the measured. We will come back to this point later.

The peak value of computed neutron yield increases from 20 to 33 kV with the same trend as the measured data. At higher charging voltage, peak value of neutron yield shifts to higher operating pressure for the measured results.

Table 3 Summary of steps to configure the neutron yield from UMDPF2 operated at different voltages

Optimization steps	Z_0 (cm)	V_0 (kV)	a (cm)	b (cm)
1	8.5	20	1.25	3.25
2	8.5	27	1.25	3.25
3	8.5	33	1.25	3.25

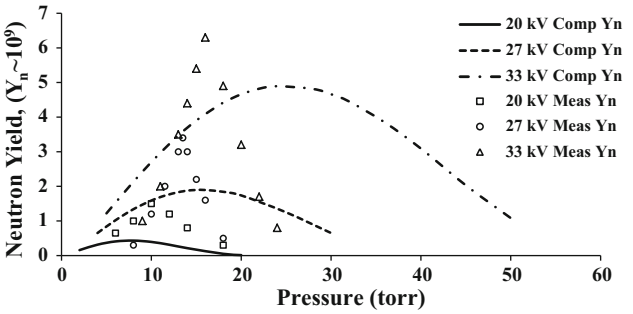

Fig. 3 Computed neutron yield versus pressure compared with measured data of UMDPF2

Similar features were exhibited in the numerical results. A narrower operating pressure regime for neutron yield was obtained experimentally whereas numerical calculations show a broader pressure regime for the neutron emission. The drop-off of neutron yield on both sides of the optimum pressure is more gradual for the computed curve than the measured curve and thus results in a much broader operating pressure range in the computed curve similar to the case of UMDPF1.

From the overall results of the numerical experiment for both machines, the computed yield shows a broader yield-vs-pressure curve especially on the higher pressure side. This is likely due to the non-inclusion of Magnetic Reynold Number MNR effects [40] in the model which comes into play at lower speeds (higher pressure beyond the time-matched regime) resulting in diffused current sheath structures and poorer performance of the electromagnetic drive mechanism. Similar trend of neutron yield versus pressure curve has also been reported by Saw et al. [41] on the computation of neutron yield at different operating pressures using Lee model code. Recently, numerical experiments on the neutron yield from PF-1000 operated at 1 MJ using the same model code has been reported and the results showed reasonable agreement with the measured results [42]. It is also worthwhile to mention the numerical experiments performed on PF-400 and FN-II [26]. Numerical results showed that both plasma focus device even operated in different range of energy but the computed neutron yield versus pressure curve still showed degrees of agreement with the laboratory measurement.

However, in several cases the computed optimum yield is lower than the measured optimum yield by a factor of up to 1/3. This is also the case for the worst divergence of our computed optimum yield for the UMDPF2 which is 1/3 of the measured optimum yield in the case of the series at 20 kV. We may then ask the question: Does this divergence of computed optimum yield being only 1/3 of the measured yield in one series out of three (the other two

having less divergence) mean that the code is not reliable for estimation of neutron yield? For this we need to discuss what the state- of- the- art is in terms of neutron yield computation. We already discussed the inconsistencies of earlier work in neutron estimations by Potter [23]. Moreno et al. [24] and Gonzalez et al. [25] were able to achieve better agreement by adjusting their axial and radial mass swept-up factors *until the computed neutron yield agree with the measured neutron yield*. Such an approach will of course give agreement, but has no predictive value. They achieved agreement despite over-estimating their radial shock speeds by a factor of two, hence shock temperatures by a factor of 4 and thermalized fusion cross-sections by a factor of 1000 [26, 41]. A more recent paper of Gonzalez et al. [43] used Von Karman approximations of radial velocity and density profiles with four parameters namely axial shape parameter, radial shape parameter, velocity profile exponent and density profile exponent *which are fitted to the measured neutron yield versus pressure curve* of the seven machines they examined using a thermonuclear mechanism. There is no mention in the paper of testing any other results of the modelling against measured experiment; nor of any predictive capabilities of the model in respect of any property or any other machine even for neutron yield. Thus, these papers by Moreno et al. and Gonzalez et al. do not estimate the neutron yield of a given plasma focus. However, in 2012 Schmidt et al. [44] used a fully kinetic simulation of dense plasma focus to obtain detail distributions of dynamics, flow and field patterns; and used the computed electric fields, temperatures and densities to estimate the neutron yield of a machine. Their estimated neutron yield turns out to be between 1/2 and 1/3 of the measured yield of the corresponding machine for one particularly condition. We are not able to find any better computations of neutron yield in the literature. Thus the one point result of Schmidt et al. and our extensive results (even the worst case of UMDPF2 at 20 kV), may be considered to be the state-of-the-art.

Conclusions

In this paper, we had demonstrated the computation of neutron yield versus pressure curve for a 12 kJ plasma focus device from two machines, namely UMDPF1 and UMDPF2 using the Lee model code. This adds to the confidence that the neutron yield computed is realistic. This also indicates the versatility of the code to examine the behaviour of the neutron yield versus pressure at different plasma focus device other than computing the optimum neutron yield only.

Apart from the realistic neutron yield, the plasma dynamics and focus properties also appear to be reliable from the computation using Lee model code with the need of only fitting the computed current waveform against measured current waveform. The model, upon a good fit of the discharge current waveforms, estimates the neutron yield due to beam-gas target mechanism. Thus, the comparison with measured data will give an indication of the component of neutron due to this production mechanism. With confidence to compare with experimental measurements, a compilation of the computed I_{pinch} and the neutron yield will establish a scaling curve for neutron yield versus pinch current.

Acknowledgments This paper is dedicated to the meticulous work of the late Dr. Chen You Hor, which has contributed greatly to the progress of plasma focus work in Malaysia. The University of Malaya Plasma Focus Laboratory acknowledges the contribution of the Juelich I capacitor bank donated through the Alexander von Humboldt Foundation in connection with the AVH Research Fellowship awarded in 1975 to one of us (LS). This capacitor bank had contributed greatly to dense plasma studies in our Laboratory. The authors are thankful to the grant support from University of Malaya: UM.S/625/3/HIR/43 and Ministry of Education Grant FRGS: FP056-2010B.

References

1. S. Lee et al., Am. J. Phys. **56**, 62 (1988)
2. S. Ahmad, S.S. Hussain, M. Sadiq, M. Shafiq, A. Waheed, M. Zakaullah, Plasma Phys. Control. Fusion **48**, 745 (2006)
3. A. Bernard, P. Cloth, H. Conrads, A. Coudeville, G. Gourlan, A. Jolas, C. Maisonnier, J.P. Rager, Nucl. Instrum. Methods **145**, 191 (1977)
4. L.K. Lim, S.L. Yap, C.S. Wong, M. Zakaullah, J. Fusion Energ. **32**, 287 (2013)
5. M.Z. Khan, S.L. Yap, Y. Ibrar, N.K. Nitturi, L.K. Lim, C.S. Wong, Sci. World J. (2014). doi:10.1155/2014/240729
6. M. Zakaullah, K. Alamgir, M. Shafiq, M. Sharif, A. Waheed, G. Murtaza, J. Fusion Energ. **19**, 143 (2000)
7. J.W. Mather, Phys. Fluids **8**, 366 (1965)
8. S. Lee, A. Serban, IEEE Trans. Plasma Sci. **24**, 1101 (1996)
9. M.J. Bernstein, F. Hai, Phys. Lett. A **31**, 317 (1970)
10. J.H. Lee, L.P. Shomo, M.D. Williams, H. Hermansdorfer, Phys. Fluids **14**, 2217 (1971)
11. S.P. Moo, C.K. Chakrabarty, S. Lee, IEEE Trans. Plasma Sci. **19**, 515 (1991)
12. S.L. Yap, C.S. Wong, P. Choi, C. Dumitrescu, S.P. Moo, Jpn. J. Appl. Phys. **44**, 8125 (2005)
13. J.H. Lee, L.P. Shomo, K.H. Kim, Phys. Fluids **15**, 2433 (1972)
14. A. Szydlowski, M. Scholz, L. Karpinski, M. Sadowski, K. Tomaszewski, M. Paduch, Nukleonika **46**, S61 (2001)
15. S. Lee, Y.H. Chen, Geometrical optimization of the dense plasma focus. Fusion Energ. IAEA-SMR **82**, 35–41 (1981)
16. A. Serban, S. Lee, J. Plasma Phys. **60**, 3 (1998)
17. J.M. Koh, R.S. Rawat, A. Patran, T. Zhang, D. Wong, S.V. Springham, T.L. Tan, S. Lee, P. Lee, Plasma Sour. Sci. Technol. **14**, 12 (2005)
18. R. Verma, R.S. Rawat, P. Lee, S. Lee, S.V. Springham, T.L. Tan, M. Krishnan, Phys. Lett. A **373**, 2568 (2009)
19. S.S. Hussain, S. Ahmad, G. Murtaza, M. Zakaullah, J. Appl. Phys. **106**, 023311 (2009)
20. B.L. Bures, M. Krishnan, R.E. Madden, F. Blobner, IEEE Trans. Plasma Sci. **38**, 667 (2010)

21. A. Talaei, S.M. Sadat, Kiai. J. Fusion Energ. **29**, 427 (2010)
22. R. Verma, R.S. Rawat, P. Lee, S.V. Springham, T.L. Tan, J. Fusion Energ. **32**, 2 (2013)
23. D.E. Potter, Phys. Fluids **14**, 1911 (1971)
24. C. Moreno, H. Bruzzone, J. Martinez, A. Clausse, IEEE Trans. Plasma Sci. **28**, 1735 (2000)
25. J. González, M. Barbaglia, F. Casanova, A. Clausse, Braz. J. Phys. **39**, 633 (2009)
26. S. Lee, S.H. Saw, L. Soto, S.V. Springham, S.P. Moo, Plasma Phys. Control. Fusion **51**, 075006 (2009)
27. S. Lee, Radiative dense plasma focus computation package: RADPF (2008). (http://www.plasmafocus.net; http://www.plasmafocus.net/IPFS/modelpackage/UPF.htm/, archival websites)
28. S. Lee, S.H. Saw, P. Lee, R.S. Rawat, Plasma Phys. Control. Fusion **51**, 105013 (2009)
29. S. Lee, S.H. Saw, J. Fusion Energ. **27**, 292 (2008)
30. S. Lee, S.H. Saw, Phys. Plasmas **19**, 112703 (2012)
31. S. Lee, S.H. Saw, Phys. Plasmas **20**, 062702 (2013)
32. M. Akel, S.A. Salo, S.H. Saw, S. Lee, J. Fusion Energ. **33**, 189 (2014)
33. Y. H. Chen, Ph.D. Thesis, University of Malaya, Kuala Lumpur, 1978
34. T. Y. Tou, Ph.D. Thesis, University of Malaya, Kuala Lumpur, 1986
35. A. Bernard et al., J. Moscow Phys. Soc. **8**, 93 (1998)
36. S. Lee, S.H. Saw, A.E. Abdou, H. Torreblanca, J. Fusion Energ. **30**, 277 (2011)
37. V.A. Gribkov et al., J. Phys. D Appl. Phys. **40**, 3592 (2007)
38. P. Cloth, H. Conrads, Nucl. Sci. Eng. **62**, 591 (1977)
39. Sh Al-Hawat, M. Akel, S. Lee, S.H. Saw, J. Fusion Energ. **31**(1), 13 (2011)
40. S. Lee, S.H. Saw, P. Lee, R.S. Rawat, K. Devi, J. Fusion Energ. **32**, 50 (2013)
41. S.H. Saw, P. Lee, R.S. Rawat, R. Verma, D. Subedi, R. Khanal, P. Gautam, R. Shrestha, A. Singh, S. Lee, J. Fusion Energ. (2014). doi:10.1007/s10894-014-9824-0
42. S.H. Saw, D. Subedi, R. Khanal, R. Shrestha, S. Dugu, S. Lee, J. Fusion Energ. **33**, 684 (2014)
43. J.H. González, F.R. Brollo, A. Clausse, IEEE Trans. Plasma Sci. **37**(11), 2178 (2009)
44. A. Schmidt, V. Tang, D. Welch, Phys. Rev. Lett. **109**(20), 205003 (2012)